Invited Paper

Synthesis and characterization of complex partially-coherent beams

Tatiana Alieva*, Alejandro Cámara and José A. Rodrigo

Universidad Complutense de Madrid, Facultad de Ciencias Físicas, Ciudad Universitaria s/n, Madrid 28040, Spain.

ABSTRACT

Partially coherent light provides attractive benefits for different applications in microscopy, astronomy, telecommunications, optical lithography, etc. However, design and generation of partially coherent beams with desirable properties is challenging. Moreover, the experimental characterization of the spatial coherence is a difficult problem involving second-order statistics represented by four-dimensional functions that cannot be directly measured and analyzed. We discuss the techniques for design and generation of partially coherent structurally stable beams and the recently developed phase-space tomography methods supported by simple experimental setups for practical quantitative characterization of partially coherent light spatial structure, including its local coherence properties.

Keywords: Partially coherent light, Phase space tomography, Statistical optics, Wigner distribution.

1. INTRODUCTION

Partially coherent light is demanded for numerous applications in microscopy, astronomy, telecommunications, and optical lithography to name a few. A part from being more robust under the propagation through random media the partially coherent light provides additional degrees of freedom for information encoding and decoding. The development of computational optics has opened the way for engineering of light coherence state, that, in general, include the control of temporal and spatial correlations and polarization yielding to very complex light structure.

In parallel to design and generation of partially coherent beams with desired form and propagation behavior different methods for their analysis have been created. Note that the coherence characterization is a rather difficult problem because even in the scalar quasi-monochromatic case a two-dimensional (2D) beam is described in paraxial approximation by a complex-valued function of four variables, $\Gamma(\mathbf{r}_1,\mathbf{r}_2)=\langle f(\mathbf{r}_1) f^*(\mathbf{r}_2)\rangle$ referenced below as a mutual intensity (MI). Here $\mathbf{r}=[x,y]^t$ is a position vector at the plane perpendicular to the beam propagation direction, $f(\mathbf{r})$ is a complex field amplitude and $\langle\cdot\rangle$ stands for ensemble averaging. Often its normalized version, $\gamma(\mathbf{r}_1,\mathbf{r}_2)=\Gamma(\mathbf{r}_1,\mathbf{r}_2)/\sqrt{\Gamma(\mathbf{r}_1,\mathbf{r}_1)\Gamma(\mathbf{r}_2,\mathbf{r}_2)}$ - the complex degree of spatial coherence, is considered. For completely coherent field the MI is reduced to the product $f(\mathbf{r}_1) f^*(\mathbf{r}_2)$ and the problem is converted into phase retrieval. It is easy to see that only the value $\Gamma(\mathbf{r},\mathbf{r})$ corresponding to the intensity distribution can be measured directly. Alternatively, the Fourier transforms of the MI: Wigner distribution (WD), $W_f(\mathbf{r},\mathbf{p})$, (see, for example, the review[1] and the references therein) and Ambiguity function (AF), $A_f(\mathbf{r},\mathbf{p})$,[2–4] respectively

$$W_f(\mathbf{r},\mathbf{p}) = \frac{1}{s^2}\int \mathrm{d}\mathbf{r}'\Gamma(\mathbf{r}+\mathbf{r}'/2,\mathbf{r}-\mathbf{r}'/2)\exp\left(-\mathrm{i}2\pi\mathbf{p}^t\mathbf{r}'/s^2\right), \quad (1)$$

$$A_f(\mathbf{r},\mathbf{p}) = \frac{1}{s^2}\int \mathrm{d}\mathbf{r}'\Gamma(\mathbf{r}+\mathbf{r}'/2,\mathbf{r}-\mathbf{r}'/2)\exp\left(-\mathrm{i}2\pi\mathbf{p}^t\mathbf{r}/s^2\right) \quad (2)$$

are used for coherence analysis. Here $\mathbf{p}=[u,v]^t$ is a vector proportional to the spatial frequency with units of length and s is a scaling factor with units of length used for proper function presentation. However, as well as the MI, neither of these functions can be directly measured. The complexity of the problem increases in the case of practical applications of beam analysis, because they usually require: Quantitative characterization of

*E-mail: talieva@fis.ucm.es

Photonic Instrumentation Engineering II, edited by Yakov G. Soskind, Craig Olson,
Proc. of SPIE Vol. 9369, 93690K · © 2015 SPIE · CCC code: 0277-786X/15/$18
doi: 10.1117/12.2083773

the spatial coherence state in the absence of a priori information about beam properties and fast acquisition as well as processing of the experimental data.

In this work we discuss different strategies for synthesis and analysis of spatial structure of scalar quasi-monochromatic partially coherent beams described by Gaussian statistics.

2. SYNTHESIS OF STABLE AND SPIRAL PARTIALLY COHERENT BEAMS

While there are different methods for synthesis of coherent beams with desired structural properties and their further generation using computer generated holograms (CGHs), their generalization to the partially coherent case is challenging. The simplest case is a generation of Schell model beams (SMBs) whose MI has a form $\Gamma(\mathbf{r}_1, \mathbf{r}_2) = \gamma(\mathbf{r}_1 - \mathbf{r}_2) f(\mathbf{r}_1) f^*(\mathbf{r}_2)$, where $\gamma(\mathbf{r})$ is the complex degree of spatial coherence defined above. The SMB can be obtained by illuminating of the CGH which encodes $f(\mathbf{r})$ with a partially coherent plane wave characterized by $\gamma(\mathbf{r})$ created from spatially incoherent light source according to the Van Cittert-Zernike theorem.[5] Such beams maintain a similar spatial structure as their coherent counterparts described by the complex field amplitude $f(\mathbf{r})$, but have reduced speckle noise. The SMBs have been found useful for certain applications in microscopy and lithography. However, they (except a Gaussian case) are not stable during propagation for a long distance even if the coherent beam associated with $f(\mathbf{r})$ is (see, for example,[6]). Here the stability means that a beam does not change the form of its intensity distribution, except of the possible scaling and rotation during propagation through homogeneous media and rotationally invariant systems. The beams whose intensity distribution rotates during the propagation are referred to as spiral beams. The beam stability is a desirable property for optical free-space communication, astronomy and other applications.

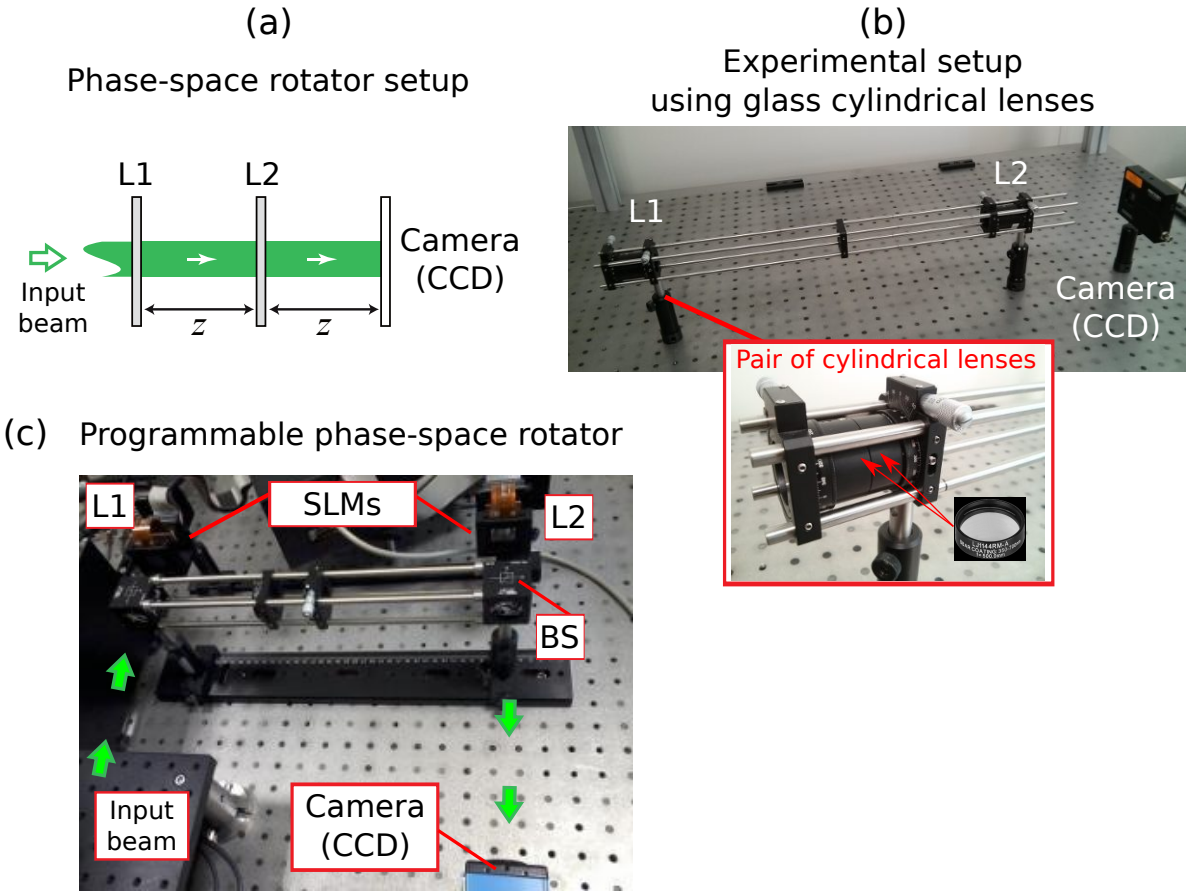

Fig. 1. (a) A general scheme for acquisition of the WD projections. (b) Experimental setup with cylindrical glass lenses. (c) Experimental setup with digital lenses implemented by spatial light modulators.

In order to design the partially coherent stable and spiral beams (pSTBs and pSPBs, respectively) it is useful to express the MI as a superposition of orthogonal mutually incoherent modes $\{\psi_n(\mathbf{r})\}$[7]as

$$\Gamma(\mathbf{r}_1, \mathbf{r}_2) = \sum_n a_n \psi_n(\mathbf{r}_1) \psi_n^*(\mathbf{r}_2), \tag{3}$$

where a_n are real non-negative constants. It is easy to see that if the set $\{\psi_n(\mathbf{r})\}$ is composed by stable modes, then the MI does not change its form a part from possible scaling and quadratic phase during its propagation. There are many sets, for example, Hermite-Gaussian (HG), Laguerre-Gaussian (LG), Hermite-Laguerre-Gaussian (HLG) o Ince-Gaussian (IG) ones, that can be used for pSTBs design. We underline that all these modes are eigenfunctions of the symmetric fractional Fourier transform (FrFT)[3,8,9] and therefore their complex field amplitude does not change during propagation in free space a part from scaling and quadratic phase modulation. Indeed, choosing an appropriate mode set, a number of modes and weights a_n a pSTB with desirable intensity, orbital angular momentum, degree of coherence can be constructed. In particular, it has been shown in[10] that the MI of the Gaussian SMB can be decomposed in HG, LG or HLG modes depending on its orbital angular momentum. Partially coherent vortex beams with a separable helicoidal phase have been synthesized[11] using the LG modes with the same topological charge as functions $\psi_n(\mathbf{r})$. Another example corresponds to incoherent sum of two complex conjugated vortex LG modes with opposite signs of the topological charge l. If $a_1 = a_2 = 1/2$ then the obtained pSTB has the same intensity distribution as the used LG modes but its coherence degree written in the polar coordinates is expressed by $\gamma(r_1, \theta_1; r_2, \theta_2) = \cos[l(\vartheta_1 - \theta_2)]$. Thus, the field at two point with the same angular coordinate θ is coherent, $|\gamma| = 1$. However, the field at the points such that $(\vartheta_1 - \theta_2)/l = \pi/2 + \pi k$ is uncorrelated. Analogously, using three LG modes the pSTB with flatten profile and rather complex coherence relation has been obtained.[6]

Applying this approach to orthogonal coherent spiral beams the pSPBs can be synthesized. We recall that a coherent spiral beam can be constructed as a coherent superposition of LG modes whose radial index p and topological charge l satisfy the expression:[12,13] $2p + l(1 + \upsilon) = \text{const}$. Here the absolute value of the rational parameter υ defines the velocity of the intensity rotation (number of loops) during beam propagation through the symmetric FrFT system in the angle interval of 2π, while the sign of υ indicates the rotation direction. Then the incoherent combination of orthogonal spiral beams with the same parameter υ corresponds to a pSPB. Note that the incoherent addition of orthogonal coherent stable beam to the pSPB does not change the rotation behavior of the final beam.

For experimental generation of pSTBs and pSPBs composed by a few orthogonal modes spatial or temporal hologram multiplexing can be used. In the first case N mutually incoherent beams are combined after being modulated by the hologram encoded the mode $\psi_n(\mathbf{r})$ (here $n = 1, 2, ...N$). In the second case the holograms encoded the modes are implemented consequently using the same SLM. Note that the time of exposition of N holograms has to be shorter than the temporal response of the system which use the synthesized partially coherent beams.

3. CHARACTERIZATION OF PARTIALLY-COHERENT BEAMS

As we have mentioned above the complete characterization of scalar paraxial quasi-monochromatic partially coherent beam requires the reconstruction of at least one of the 4D functions: MI, WD or AF. Since they cannot be measured directly (MI and AF are in general complex-valued and the WD is a real function, but can take negative values) the interferometric or diffraction methods are used for this purpose. The input data for the reconstruction process is a set of 2D intensity distributions. For the reconstruction of the 4D function other two independent parameters are required. To demonstrate the complexity of the problem consider the reconstruction of one of these 4D functions sampled in a grid of $N \times N \times N \times N$ points with double precision (8 B per sampling point). In this situation, 32 GiB are required only to store the resulting function with $N = 256$. Moreover, this excessive amount of information has to be registered and processed for the function recovery and its analysis.

Different techniques have been developed in the last decades[14–23] yet none has demonstrated to be feasible for quantitative estimation of the coherence properties of a general beam. Some methods assume certain hypothesis about light-field model,[14–16] its symmetry[17,24] or coherence properties.[22,25] Others apply pinhole or

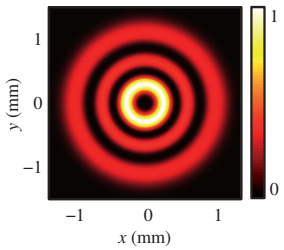

Fig. 2. The coinciding intensity distribution of the LG mode and the pSTB.

slit masks[20–22] which alter the measurements and decrease the signal to noise ratio caused by significant power reduction of the analyzed field. The phase-space tomography method[23] avoid this drawback. Moreover, it allows characterizing a beam without any a priory information about its coherence state as well as can take into account the beam symmetry discovered during data acquisition. Phase-space tomography is based on the rotation of the WD (and also the AF) after the beam propagation through ABCD systems and the measurements of the 2D WD projections, which correspond to the intensity distributions at the output of these systems.[3,26] Nevertheless, it has not been widely used for coherence analysis so far due to three principal reasons: the absence of a setup for rapid acquisition of the required experimental data and the inherent difficulties of reconstructing and analyzing the resulting 4D functions associated to the light coherence information. Recently we have proposed two experimental setups which allow automatized acquisition of the WD projections.[24,27–30] Here we discuss the question about what measured data are sufficient for beam characterization and how it can be optimally acquired.

All possible rotations in the phase space $(\mathbf{r}-\mathbf{p})$ can be described by the cascade of the three operators: $\mathbf{T}_R^{\beta}\mathbf{T}_F^{\gamma_x,\gamma_y}\mathbf{T}_R^{\alpha}$. Here $\mathbf{T}_F^{\gamma_x,\gamma_y}$ is the 2D fractional Fourier transform (FrFT) for angles γ_x and γ_y (corresponding to the WD rotation in planes $x-p_x$ and $y-p_y$) and $\mathbf{T}_R^{\alpha}$ is the rotation operator for angle α in the plane transverse to beam propagation ($x-y$ and p_x-p_y).[3,9,30] The FrFT is called symmetric and antisymmetric if $\gamma_x=\gamma_y=\gamma$ and $\gamma_x=-\gamma_y=\gamma$, respectively. Since the WD projection, $P^{\beta,\gamma_x,\gamma_y,\alpha}(\mathbf{r})$, is a 2D function of spatial coordinates $\mathbf{r}$, then only two of the four parameters, γ_x, γ_y, α and β, independently changing in a π-interval, are required for the WD (and therefore the AI and the MI) recovery. Note that the rotation at angle β can be done digitally after the projection acquisition.

The choice of the projection set is on the first turn restricted by the available setup. A general scheme of optical setup which provides the acquisition of all possible WD projection is shown in Fig. 1(a). It comprises two generalized lenses, each of which is a combination of two cylindrical lenses, and a digital camera. The positions of all elements are fixed. The appropriate change of the power of the cylindrical lenses and the relative rotation of their axis allow obtaining a desired WD projection. However, the requirement of the fast acquisition of a big number of projections impedes the use of glass lenses of different power. On the other hand, the application of the cylindrical lenses of fixed power limits the set of projections $\left\{P^{\beta,\gamma,-\gamma,\alpha}(\mathbf{r})\right\}$ which can be registered by the setup (see, Fig. 1(b)). The change of the angles in this case is obtained by lens (and if necessary image) rotations - the process which can be easily automatized. However, the further recovery of the WD and the analysis of the field correlations from this set require significant computational efforts. Then its application is more appropriate for the beams which have a certain symmetry that allows reducing the set of the projections $\left\{P^{0,\gamma,-\gamma,0}(\mathbf{r})\right\}$ and simplifying the reconstruction process. Thus it has been shown in[24,31] that this set is sufficient for the characterization of partially coherent beams separable in Cartesian coordinates whose MI is written in the form $\Gamma(\mathbf{r}_1,\mathbf{r}_2)=\Gamma_x(x_1,x_2)\Gamma_y(y_1,y_2)$. Moreover, the same projection set can be used for confirmation of the hypothesis of beam separability.

Another type of the beams which can be completely characterized by the set of projections associated with the antisymmetric FrFT is described by rotationally symmetric MI. The MI of such rotationally symmetric beams (RSBs) satisfies the following condition: $\Gamma(\mathbf{r}_1,\mathbf{r}_2)=\Gamma(\mathbf{M}(\theta)\mathbf{r}_1,\mathbf{M}(\theta)\mathbf{r}_2)$ for any angle θ, where

$$\mathbf{M}(\theta)=\begin{bmatrix}\cos\theta & -\sin\theta\\ \sin\theta & \cos\theta\end{bmatrix}.$$

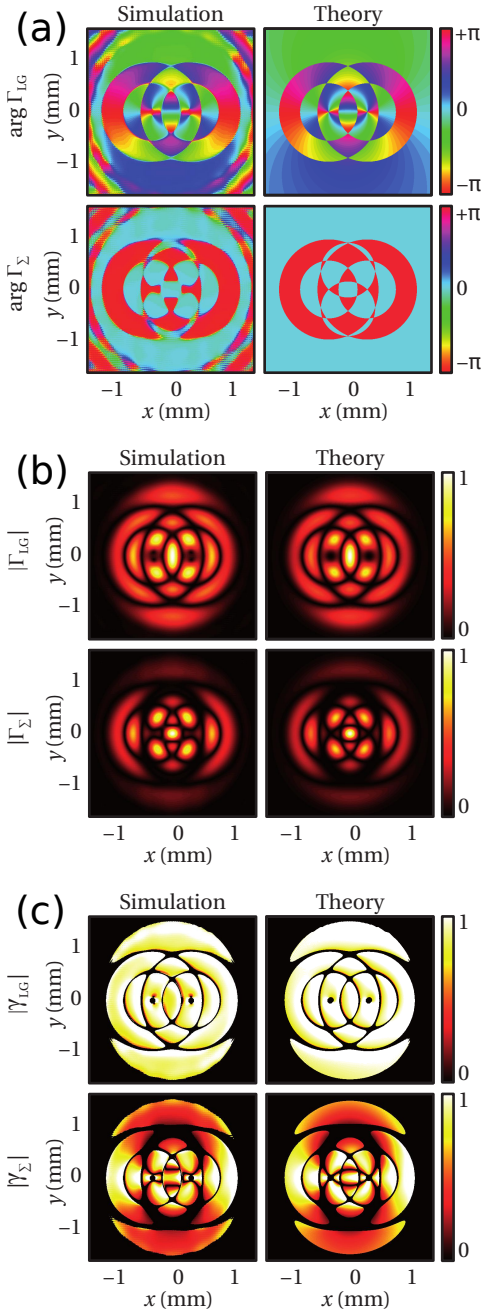

Fig. 3. Simulated (the first column) and theoretically predicted (the second column) phase (a), modulus (b) and normalized modulus (degree of coherence) (c) of the MI of the LG mode, $\Gamma_{LG}(\mathbf{r}+\mathbf{r}_0/2, \mathbf{r}-\mathbf{r}_0/2)$, (the first row) and of the pSTB, $\Gamma_{\Sigma}(\mathbf{r}+\mathbf{r}_0/2, \mathbf{r}-\mathbf{r}_0/2)$, (the second row) for the reference point $\mathbf{r}_0 = (0.55, 0)$mm.

Although it is not a property exclusive to RSBs, all of them present an intensity distribution that is rotationally invariant. Coherent and partially coherent vortex beams are the more important subclass of the RSBs. The rotational symmetry of the MI (and therefore the WD and AI) can be checked from the simple analysis of WD projections associated with the antisymmetric FrFT.[4,31] If the test fails then the complete set of the projections $\left\{P^{\beta,\gamma,-\gamma,\alpha}(\mathbf{r})\right\}$ has to be used for beam analysis. The procedure of the reconstruction of the MI of the RSBs and its experimental verification can be found in,[4,31] here we demonstrate the results of its application to the pSTB discussed in Section 2. The pSTB is constructed as incoherent superposition of LG modes with the same

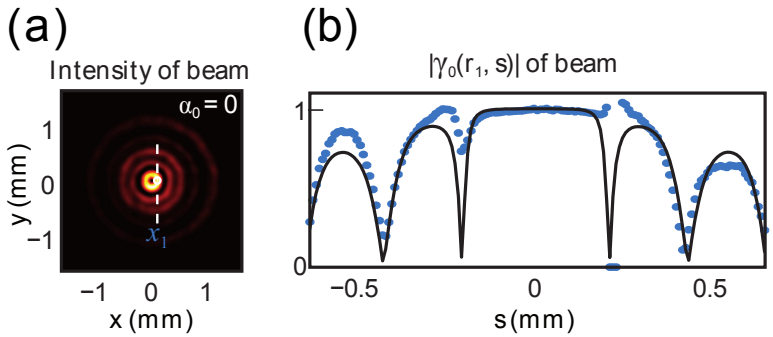

Fig. 4. (a) Intensity distribution of the studied pSTB. (b) Experimentally recovered (dashed blue line) and theoretically predicted (solid black line) modulus of the degree of coherence associated to the pSTB, $|\gamma(\mathbf{r}_1, s)|$ for $\alpha_0 = 0$ and $\mathbf{r}_1 = (x_1, 0) = (0.12, 0)$mm.

radial index $p = 2$ and the opposite topological charge of modulus $|l| = 2$. The weights of both modes are equal that means that the intensity distribution of the partially coherent beam is indistinguishable from the intensity distribution of any of these modes (see, Fig. 2). However, the MIs of the beams are significantly different:

$$\Gamma_{LG}(\mathbf{r}_1, \mathbf{r}_2) = LG_2^2(\mathbf{r}_1) \left[LG_2^2(\mathbf{r}_2)\right]^* \exp\left[2\left(\vartheta_1 - \theta_2\right)\right], \quad (4)$$

$$\Gamma_{\Sigma}(\mathbf{r}_1, \mathbf{r}_2) = LG_2^2(\mathbf{r}_1) \left[LG_2^2(\mathbf{r}_2)\right]^* \cos\left[2\left(\vartheta_1 - \theta_2\right)\right]. \quad (5)$$

The MI of the LG mode and of the associated pSTB have been reconstructed from 90 simulated WD projections associated with antisymmetric FrFT (following the phase space tomography method proposed in[4]). They are compared with the theoretically calculated ones in Fig. 3. In particular, the Fig. 3(a) corresponds to the MI phase and the Fig. 3(b) corresponds to the MI modulus, while in the Fig. 3(c) the modulus of the coherence degree is displayed. The good matching between the simulated and theoretically calculated beam coherence characteristics verify the method applicability. We underline that not only the modulus but also the phase of the MI are reconstructed. It is easy to see from the Fig. 3(c) that the field in the reference point is completely correlated with the field in any other point (where the intensity distribution is not zero) in the case of the coherent LG mode, while in the case of pSTB it occurs only for the points from the line of the same azimuthal angle, $x = 0$, according to Eq. 5.

Note that other type of a priory information about partially coherent beam, for example a small number of the MI modes, also allows using the reduced projection set for beam characterization and in additon applying the compressive phase space tomography technique proposed in.[25]

In the case when there is no a priori information about the beam coherence state the set of projections for two independent angles has to be used. As we have mentioned before in order to measure the projection which does not belong to set $\left\{P^{\beta,\gamma,-\gamma,\alpha}(\mathbf{r})\right\}$ using the setup with fixed elements positions from Fig. 1(a), we need to change the lens power. This can be done easily if the lenses are digitally implemented by spatial light modulators. The photograph of such experimental system developed in our laboratory[27] is shown in Fig. 1(c). While this setup allows automatized video-rate measuring of any projection set suitable for the WD reconstruction (for example one which we have discussed above or the set $\left\{P^{0,\gamma_x,\gamma_y,0}(\mathbf{r})\right\}$ corresponding to the FrFT used in[23]) there is a set which is more appropriate for practical application of the phase space tomography. This set, $\left\{P^{0,0,\gamma,\alpha}(\mathbf{r})\right\}$, as it has been demonstrated in[32] allows simultaneous performing of the data acquisition and processing. Since every projection subset for a fixed angle α_0 is an independent entity, then the WD and the MI of the optical field at the points along the parallel lines which form angle α_0 with the axes y can be obtained from this subset. This allows starting the beam analysis before the complete projection set is acquired. Moreover, as one projection subset slice $\left\{P^{0,0,\gamma,\alpha_0}(x_0, y)\right\}$ is independent of the rest, the data processing is inherently prepared for parallel computing.

For experimental demonstration of this method the pSTB composed by two mutually incoherent LG modes LG_0^3 and LG_4^1 with the weights 3/4 and 1/4 correspondingly has been generated by temporal hologram multiplexing. Measuring 180 projections of the subset $\left\{P^{0,0,\gamma,\alpha_0}(x_0, y)\right\}$ for $\alpha_0 = 0$ and γ ranging in $(\pi/2, 3\pi/2)$

the MI and the degree of coherence of the field between the points belonging to the same vertical line have been recovered. In Fig. 4(a) the intensity distribution of the generated beam is displayed. The experimentally retrieved (dashed blue line) and theoretically predicted (solid black line) moduli of the degree of coherence are shown in Fig. 4(b). The rather complicated curve described the $|\gamma|$ is well recovered from the experimental data. The small disagreement between two curves is explained by the deviations of the generated pSTB (due to the hologram encoding) from the theoretical one.

4. CONCLUSIONS

The further application of partially coherent light will certainly require the encoding and decoding the information it carries on. We have considered the methods of synthesis and generation of partially coherent stable and spiral beams which have the potential application for free-space communication and atmosphere monitoring. Several phase space tomography techniques suitable for practical quantitative analysis of partially coherent beams have been discussed. The diversity of the WD projection sets allows using various lens configurations and different reconstruction algorithms for beam characterization. While some of them can be applied to a priori unknown beams, others are sustained by hypotheses about the beam symmetry o its coherence model that simplify and accelerate the MI reconstruction process. The incorporation of high-speed digital cameras and spatial light phase modulators for digital lens implementation as well as electromechanical devices for cylindrical glass lens rotation in the discussed experimental setups will further increase the benefits of these techniques.

ACKNOWLEDGMENTS

Spanish *Ministerio de Economía y Competitividad* is acknowledged for funding the project TEC2011-23629.

REFERENCES

1. Alonso, M. A., "Wigner functions in optics: describing beams as ray bundles and pulses as particle ensembles," *Adv. Opt. Photon.* **3**(4), 272–365 (2011).
2. Tu, J. and Tamura, S., "Wave field determination using tomography of the ambiguity function," *Phys. Rev. E* **55**(2), 1946–1949 (1997).
3. Hennelly, B., Ojeda-Castañeda, J., and Testorf, M., eds., [*Phase Space Optics: Fundamentals and Applications*], McGraw-Hil (2009).
4. Cámara, A., Alieva, T., Castro, I., and Rodrigo, J. A., "Phase-space tomography for characterization of rotationally symmetric beams," *J. Opt.* **16**(1), 015705 (2014).
5. Goodman, J. W., [*Statistical Optics*], Wiley&Sons, NY (2000).
6. Alieva, T., Rodrigo, J. A., Cámara, A., and Abramochkin, E., "Partially coherent stable and spiral beams," *J. Opt. Soc. Am. A* **30**(11), 2237–2243 (2013).
7. Mandel, L. and Wolf, E., [*Optical Coherence and Quantum Optics*], Cambridge University Press, New York (1995).
8. Ozaktas, H. M., Zalevsky, Z., and Kutay, M. A., [*The Fractional Fourier Transform with Applications in Optics and Signal Processing*], John Wiley&Sons, NY, USA (2001).
9. Alieva, T., [*Advances in Information Optics and Photonics, ICO International Trends in Optics: Vol. VI*], ch. First-Order Optical Systems for Information Processing, 1–26, SPIE Press, USA (2008).
10. Sundar, K., Mukunda, N., and Simon, R., "Coherent-mode decomposition of general anisotropic Gaussian Schell-model beams," *J. Opt. Soc. Am. A* **12**(3), 560–569 (1995).
11. Ponomarenko, S. A., "A class of partially coherent beams carrying optical vortices," *J. Opt. Soc. Am. A* **18**(1), 150–156 (2001).
12. Piestun, R. and Shamir, J., "Generalized propagation-invariant wave fields," *J. Opt. Soc. Am. A* **15**, 3039–3044 (Dec 1998).
13. Alieva, T., Abramochkin, E., Asenjo-Garcia, A., and Razueva, E., "Rotating beams in isotropic optical system," *Opt. Express* **18**(4), 3568–3573 (2010).
14. Alieva, T. and Agullo-Lopez, F., "Reconstruction of the optical correlation function in a quadratic refractive index medium," *Opt. Commun.* **114**, 161–169 (1995).

15. Tran, C. Q. and Nugent, K. A., "Recovering the complete coherence function of a generalized Schell model field," *Opt. Lett.* **31**(22), 3226–3227 (2006).
16. Gureyev, T. E., Roberts, A., and Nugent, K. A., "Partially coherent fields, the transport-of-intensity equation, and phase uniqueness," *J. Opt. Soc. Am. A* **12**(9), 1942–1946 (1995).
17. Agarwal, G. S. and Simon, R., "Reconstruction of the Wigner transform of a rotationally symmetric two-dimensional beam from the Wigner transform of the beam's one-dimensional sample," *Opt. Lett.* **25**(18), 1379–1381 (2000).
18. Cámara, A., Alieva, T., Rodrigo, J. A., and Calvo, M. L., "Phase space tomography reconstruction of the wigner distribution for optical beams separable in cartesian coordinates," *J. Opt. Soc. Am. A* **26**(6), 1301–1306 (2009).
19. Nugent, K. A., "Partially coherent diffraction patterns and coherence measurement," *J. Opt. Soc. Am. A* **8**, 1574–1579 (Oct 1991).
20. Santarsiero, M. and Borghi, R., "Measuring spatial coherence by using a reversed-wavefront Young interferometer," *Opt. Lett.* **31**(7), 861–863 (2006).
21. González, A. I. and Mejía, Y., "Nonredundant array of apertures to measure the spatial coherence in two dimensions with only one interferogram," *J. Opt. Soc. Am. A* **28**(6), 1107–1113 (2011).
22. Waller, L., Situ, G., and Fleischer, J. W., "Phase-space measurement and coherence synthesis of optical beams," *Nature Photon.* **6**(7), 474–479 (2012).
23. Raymer, M. G., Beck, M., and McAlister, D. F., "Complex wave-field reconstruction usign phase-space tomography," *Phys. Rev. Lett.* **72**(8), 1137–1140 (1994).
24. Cámara, A., Alieva, T., Rodrigo, J. A., and Calvo, M. L., "Phase space tomography reconstruction of the Wigner distribution for optical beams separable in Cartesian coordinates," *J. Opt. Soc. Am. A* **26**(6), 1301–1306 (2009).
25. Tian, L., Lee, J., Oh, S. B., and Barbastathis, G., "Experimental compressive phase space tomography," *Opt. Express* **20**(8), 8296–8308 (2012).
26. Alieva, T., Cámara, A., Rodrigo, J. A., and Calvo, M. L., [*Optical and Digital Image Processing*], ch. Phase-space tomography of optical beams, Wiley-VCH (2011).
27. Rodrigo, J. A., Alieva, T., and Calvo, M. L., "Programmable two-dimensional optical fractional Fourier processor," *Opt. Express* **17**(7), 4976–4983 (2009).
28. Rodrigo, J. A., Alieva, T., and Calvo, M. L., "Experimental implementation of the gyrator transform," *J. Opt. Soc. Am. A* **24**(10), 3135–3139 (2007).
29. Rodrigo, J. A., *First-order optical systems in information processing and optronic devices*, PhD thesis, Universidad Complutense de Madrid (2008).
30. Rodrigo, J. A., Alieva, T., and Bastiaans, M. J., [*Optical and digital image processing*], ch. 12, Wiley-VCH Verlag Berlin (2011).
31. Cámara, A., *Optical beam characterisation via phase-space tomography*, PhD thesis, Universidad Complutense de Madrid (2014).
32. Cámara, A., Rodrigo, J. A., and Alieva, T., "Optical coherenscopy based on phase-space tomography," *Opt. Express* **21**(11), 13169–13183 (2013).